Accurate Measurement of Nanofluid Thermal Conductivity By Use of a Polysaccharide Stabilising Agent[☆]

R. Ebrahimi[a], D. de Faoite[a], D. P. Finn[a], K. T. Stanton[a,*]

[a]School of Mechanical and Materials Engineering, University College Dublin, Ireland

Abstract

Measuring the thermal conductivity of low viscosity fluids such as aqueous nanofluids is challenging due to the formation of convection currents. In the current work, a modification of the transient hot-wire thermal conductivity measurement technique was investigated to address this problem. The polysaccharide agar was used as a gelling agent to prevent the formation of convection currents, thereby enabling measurement of thermal conductivity. The experimental method was validated by comparison of experimentally measured thermal conductivity values with published reference values over a range of temperatures for two reference fluids stabilised by agar: water and an ethylene glycol/water solution. The precision of thermal conductivity measurements was found to be significantly improved by use of this gelling agent. These findings indicate that agar, or a similar gelling agent, can be used to enable accurate measurement of the thermal conductivity of aqueous fluids. This measurement technique was utilised to accurately measure the thermal conductivity enhancements of copper and alumina aqueous nanofluids with low nanoparticle concentrations, over a range of temperatures. The thermal conductivities of these nanofluids were found to be within ± 2 % of those predicted by the Maxwell model.

Keywords: thermal conductivity, nanofluid, polysaccharide gel, agar, copper, alumina

[☆]This research was funded by the Ministry of Science, Research and Technology (Iran); University College Dublin Seed Funding Grant SF656; and the Higher Education Authority (HEA) of Ireland through the Programme for Research in Third-Level Institutions (PRTLI4).
Declarations of interest: none.

[*]Corresponding author
Email address: kenneth.stanton@ucd.ie (K. T. Stanton)

1. Introduction

Measuring the thermal conductivity of low viscosity fluids such as water or aqueous nanofluids is difficult due to the potential for formation of convection currents [1–5]. The most widely used technique for measuring the thermal conductivity of such fluids is the transient hot-wire method, which works by measuring the transient temperature field around a line-source heater [4]. The theory and experimental setup for this measurement technique are well described in the literature [1, 6–10]. A thin metallic wire (generally platinum, with a diameter of less than 100 μm) is submerged into the liquid sample. This wire acts simultaneously as a heat source and a temperature sensing element [11]. The wire is electrically heated for a short period of time, typically of the order of 1 s–3 s [1, 12]. Assuming that the surrounding fluid is initially at uniform temperature, and that the heat source approximates a line of infinite length, the fluid thermal conductivity may be calculated from the transient temperature response of the wire.

Design and construction of accurate transient hot-wire measurement apparatus is challenging. Two key design parameters are the wire thickness and heating period. The wire must be very thin to minimise its heat capacity, which would otherwise affect the transient temperature response of the wire. The heating period must be short in order to avoid formation of convection currents [1, 12]. Numerous experimental studies have used carefully designed transient hot-wire apparatus for thermal conductivity measurement of low viscosity fluids and have reported good measurement precision, and accuracies of better than ± 0.5 % [6, 8, 9, 13]. Accurate thermal conductivity measurements have similarly been made for aqueous nanofluids using such apparatus [12, 14].

Despite this, a significant proportion of studies investigating the thermal conductivity of aqueous nanofluids use commercial measurement devices based on the transient hot-wire technique, but which differ significantly in design details from conventional transient hot-wire apparatus. The most widely used of these devices is the KD2 Pro thermal analyser with KS-1 probe needle produced by Decagon Devices, Inc. (Pullman, Washington, USA). A large number of studies have used the KD2 Pro/KS-1 system for measuring the thermal conductivity of nanofluids [5, 15–25]. This device uses a short stainless steel hot-wire 'probe' with a much lower length:diameter ratio (≈ 46:1) than typical transient hot-wire apparatus (> 1000:1). Advantages of this device include

its low cost and convenience.

The heat capacity per unit length of the KS-1 probe, which has a diameter of 1.3 mm, is significantly higher than that of platinum wires traditionally used for transient hot-wire apparatus, which typically have diameters of 10 µm–50 µm. This increased heat capacity affects the probe transient temperature response and precludes the use of a very short heating period. The minimum heating period for this device is 30 s, which significantly increases the propensity for convection current formation, particularly for low viscosity fluids. Formation of convection currents around the heated probe can increase the heat transfer from the probe relative to the heat transfer caused solely by thermal diffusion in the fluid. This can lead to bias and precision errors in measured thermal conductivity values, potentially making measurements unreliable.

The current work describes a modification to the transient hot-wire thermal conductivity measurement technique that enables the thermal conductivity of low viscosity fluids to be reliably measured even when using a low length:diameter ratio probe. The key innovation is the use of the polysaccharide agar is used as a gelling agent to minimise convection heat transfer. Agar can form a gel with water and some aqueous solutions and colloids, thereby preventing convection currents from forming. Agar dissolved in water behaves as a reversible sol-gel. The structural principles of agar gel formation have been elucidated by Tako & Nakamura [26–28]. During gel formation, hydrogen bonding occurs between the polysaccharide molecules and water. Tetrahedrally directed hydrogen bonding additionally occurs between water molecules over an extended range, thereby forming a stabilised ice-like structure [28]. Above approximately 85 °C, formation of glycosidic bonds between saccharide units to form a polymeric polysaccharide results in the gelling behaviour of agar. Once cooled below approximately 40 °C a gel is formed, which is stable upon re-heating up to approximately 80 °C. Only a small quantity of agar, of the order of 0.5 wt%, needs to be added to water to form a stabilised gel. The use of agar for measurement of the thermal conductivity of liquids has been suggested by transient hot-wire instrument manufacturer Decagon Devices, Inc. (Pullman, Washington, USA) [29]. However, a rigorous assessment of this technique has not been found in the technical literature. Only a few reports of the use of agar stabilised liquids for thermal property measurement could be found. Campbell et al., Ochsner et al. and Liu, for ex-

ample, used agar stabilised water to calibrate heated probe volumetric heat capacity measurement systems [30–32].

A specific class of low viscosity fluids for which measurement of thermal conductivity is of particular technical interest is nanofluids—colloidal suspensions of solid nanoparticles dispersed in a base fluid. 'Heat transfer nanofluids' (HTNF) are a new class of coolants, for which enhancements in thermal conductivity relative to their base fluids have been reported. Nanofluids have been widely investigated for thermal applications, including heat transfer in microchannels [33, 34], automotive coolants [35], refrigerants [36], and heating, ventilation and air-conditioning (HVAC) systems [37]. Nanoparticles investigated are most commonly either metals, metal oxides, or carbon based nanostructured materials such as carbon nanotubes (CNT) [5, 38, 39]. The majority of studies have used water as the base liquid, but solutions of ethylene glycol and water (EG/W) [40], ethylene glycol (EG) [41], engine oil [42], and kerosene [43] have also been used. Efficient convective cooling is an important requirement in many industries, so enhancement of fluid thermal conductivity may benefit a wide range of industrial processes. Accurate measurement of nanofluid thermal conductivity is essential in order to assess the suitability of nanofluids for such heat transfer applications. Accurate measurement of small thermal conductivity enhancements, as may be conferred by addition of low concentrations of nanoparticles to a base fluid, is particularly challenging, and requires the use of very precise and well calibrated measurement apparatus.

According to the classical model of Maxwell, the thermal conductivity of a fluid may be increased by addition of solid particles with thermal conductivity higher than that of the base fluid [44]. Maxwell's model, which is based on the effective medium theory, predicts that the thermal conductivity for a liquid containing a dilute suspension of spherical particles is given by:

$$k_{\mathrm{n}} = k_{\mathrm{b}}\left(1 + \frac{3\phi\,(\delta - 1)}{\delta + 2 - \phi\,(\delta - 1)}\right) \tag{1}$$

where k_{b} is the thermal conductivity of the base fluid, δ is the ratio of particle to base fluid thermal conductivity ($k_{\mathrm{p}}/k_{\mathrm{b}}$), and ϕ is the volume fraction of particles [44].

A number of studies of HTNFs have reported thermal conductivity enhancements that far exceed those predicted by the Maxwell model. For instance, 40 % thermal conductivity enhancement

was reported by Eastman et al. using 0.3 vol% of copper nanoparticles [45], and a 160 % increase in thermal conductivity was reported by Choi et al. for an oil-based nanofluid containing 1 vol% of carbon nanotubes [46]. As a result of some of these very high and, according to classical theory, anomalous enhancements, heat transfer nanofluids became the subject of intense research and some controversy emerged as to the real enhancement values and possible underlying heat transfer mechanisms at the nanoscale [47]. Despite an extensive number of theoretical and experimental studies, the heat transfer mechanism in nanofluids is not yet fully understood, and the heat transfer enhancements reported for these fluids in the scientific literature vary greatly. For example, one recent round-robin study found no anomalous enhancement in thermal conductivity for HTNFs [3].

The use of agar as a stabilising agent has many advantages for the measurement of thermal conductivity of nanofluids. Particle settling over time and the movement of particles due to convection pose challenges for the experimental measurement of thermal conductivity for these fluids. Performing a number of repeat measurements of thermal conductivity at a single temperature can take several hours. Therefore, if a nanofluid is not fully stable (i.e., if particle clustering or settling occurs), the concentration of suspended nanoparticles will change over time, and the measured values of thermal conductivity will also vary. Indeed, some studies have reported a decline in nanofluid thermal conductivity with elapsed time, likely caused by nanoparticle clustering [48–51]. In contrast, stabilising by agar effectively prevents particle settling, enabling measurement of the thermal conductivity of nanofluids in the 'as-prepared' state.

In the current paper, the effectiveness of this agent for thermal conductivity measurement of liquids is assessed. The accuracy of this measurement method was verified by measuring the thermal conductivity of water and an ethylene glycol/water solution, stabilised by agar, over a range of temperatures and comparing the measured thermal conductivity values with reference values from the literature. Following verification using reference fluids, measurements of the thermal conductivity of aqueous nanofluids separately incorporating Cu and Al_2O_3 nanoparticles were then performed using this method. Copper nanofluids have previously been investigated by Eastman et al. [45] and Li et al. [52], while Al_2O_3 nanofluids have been studied by several authors (e.g. [10, 15, 53]). The apparent thermal conductivity enhancement relative to the base fluid was calculated

for these nanofluids and compared to the predictions of the Maxwell model.

2. Materials and Methods

2.1. The KD2 Pro/KS-1 Measurement System

A KD2 Pro thermal analyser with a KS-1 sensor probe (Decagon Devices, Inc., Pullman, Washington, USA), which operates based on the transient hot-wire method, was used to measure the thermal conductivity of base fluids and nanofluids. The KS-1 probe needle is 1.3 mm in diameter and 60 mm long and acts as the hot-wire and temperature sensor. The probe needle is made of stainless steel encircling a resistive heating element and temperature sensor. For each measurement, the temperature of the fluid being examined was measured using the temperature sensor in the KS-1 probe. The measurement system composed of the KD2 Pro and KS-1 probe has a specified uncertainty of $\pm 5\,\%$ of the measured value between $0.2\,\mathrm{W{\cdot}m^{-1}{\cdot}K^{-1}}$ and $2\,\mathrm{W{\cdot}m^{-1}{\cdot}K^{-1}}$ for liquids. The measurement resolution of the KD2 Pro/KS-1 measurement system is $0.001\,\mathrm{W{\cdot}m^{-1}{\cdot}K^{-1}}$. The KD2 Pro device was factory calibrated for thermal conductivity measurements against glycerol at 23 °C.

2.2. Experimental Measurement Setup

In order to maximise repeatability between experiments, a cylindrical test container was designed to hold a volume of liquid for testing and to hold the measurement probe securely in place, as shown in Figure 1. The cylindrical container was machined from 316 stainless steel, and had a 40 mm inner diameter, a 76 mm outer diameter and an internal chamber height of 80 mm. The internal chamber could hold a liquid volume of approximately 100 ml. A tight fitting slot was machined into the bottom of the container for the KS-1 probe head to fit into. The probe was located at the bottom of the chamber, radially in the middle of the chamber, and oriented vertically upward. Vertical upward placement of the probe needle minimised the potential for convection current formation in the fluid and ensured that the full length of the probe was immersed in the fluid. This orientation also allowed the test liquid to be easily poured in at the top of the chamber. The secure fixation of the probe aids in ensuring that repeatable measurements are obtained for various fluids. A top-cap was placed on top of the container, sealed by a rubber gasket to prevent

any fluid leakage. A small stainless steel vent tube was placed on the top-cap to ensure that the test liquid inside the chamber remained at ambient pressure. A similar experimental measurement setup for the KD2 Pro system, with a KS-1 probe located vertically in a measurement chamber, was used for example by Han et al. for measurement of the thermal conductivity of nanofluids [18].

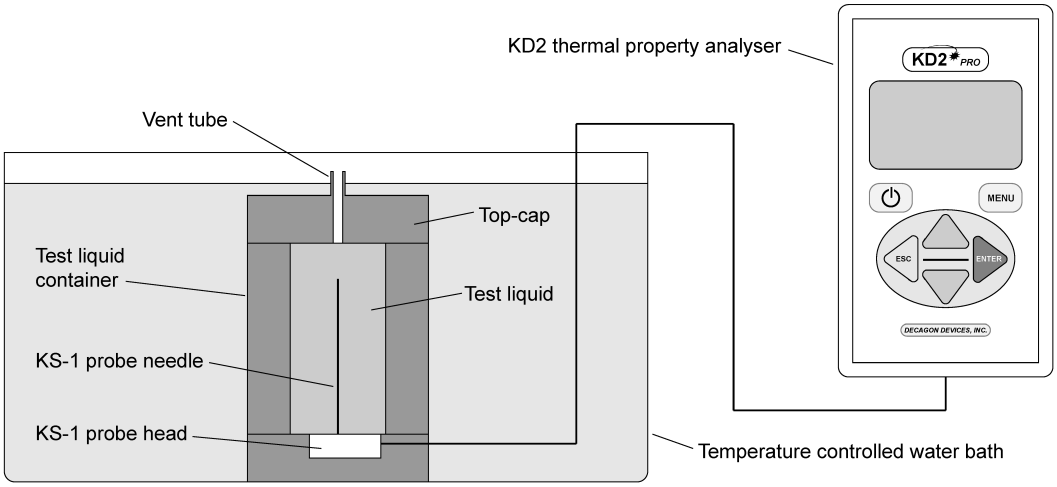

Figure 1: Experimental setup for measurement of liquid thermal conductivity using the KD2 Pro/KS-1 measurement system.

The entire assembly was placed into a Julabo F34 temperature controlled circulating water bath (Julabo GmbH, Seelbach, Germany). The temperature controlled water bath kept the temperature of the measurement chamber constant, and set the fluid temperature at which the tests were performed. In order to perform reliable measurements it is required that the fluid in the measurement chamber is kept at a constant temperature. To assess the water bath temperature stability, the water bath temperature was measured over a 60 min period. The maximum deviation from the average temperature was found to be $\pm\,0.02\,^{\circ}\mathrm{C}$, in good agreement with the temperature stability of $\pm\,0.03\,^{\circ}\mathrm{C}$ reported by the water bath manufacturer. During each individual thermal conductivity measurement, the water bath circulation pump was temporarily switched off to eliminate vibrations, which might otherwise aid in initiating convection current formation.

2.3. Experimental Procedure

The KD2 Pro instrument can be configured to operate in one of two modes: a standard 'low power mode' (LPM) or a 'high power mode' (HPM). When operated in HPM the heat input

to the probe is increased, resulting in a higher temperature rise in the probe and surrounding liquid. For deionised water, LPM results in a temperature rise in the probe of circa 0.3 °C, while HPM results in a temperature rise in the probe of circa 3.0 °C. For measurement of liquid thermal conductivity with the KD2 Pro/KS-1 system, the use of LPM is recommended by the manufacturers in order to minimise convection current formation [54]. In the current work, thermal conductivity measurements were performed using both LPM and HPM for deionised water and deionised water stabilised by agar in order to assess the effect of different heat inputs on measurement precision. HPM was used for thermal conductivity measurements of the agar stabilised ethylene glycol/water solution and agar stabilised nanofluids.

Each thermal conductivity measurement with the KD2 Pro consists of three steps. Firstly, the KD2 Pro is programmed with a delay of 30 s for the temperature of the fluid to become uniform before heating starts. Secondly, the KS-1 probe needle generates a small amount of heat internally by resistance heating for 30 s. The entire needle is heated simultaneously, and the temperature of the needle is recorded at 1 s intervals during the heating period. Thirdly, the heat generation ceases and the needle begins to cool down. The temperature of the needle is similarly recorded at 1 s intervals over a cooling period of 30 s. Subsequently, the thermal conductivity of the fluid is calculated by the KD2 Pro system from the combined needle temperature measurements recorded during heating and cooling periods.

Thermal conductivity measurements for the studied fluids were performed over a range of temperatures. At least 10 measurements were taken at each temperature. The arithmetic mean value at each temperature was then calculated. Prior to performing measurements at a given temperature, the water bath and measurement system was held at a constant temperature for 60 min to allow the system to fully isothermalise. Measurements were then performed at 15 min intervals to allow the system to re-isothermalise at the correct temperature following each test.

2.4. Verification and Calibration Method

Thermal conductivity measurements for deionised water were first performed in order to assess the measurement system without use of a stabilising agent. Measured thermal conductivity values were compared to the reference values reported by ASHRAE (the American Society of Heating,

Refrigerating and Air-Conditioning Engineers) as a means of assessing the accuracy of the experimental measurements [55].

To verify the reliability of using agar as a stabilising agent for thermal conductivity measurements, agar stabilised deionised water and an agar stabilised ethylene glycol/water (EG/W) solution were tested using the same procedure. The EG/W solution chosen for testing contained 10 vol% ethylene glycol, as solutions near this concentration range are commonly used as coolants in refrigeration systems [56]. Measured thermal conductivity values for 10 vol% ethylene glycol/water were compared to the reference values reported by ASHRAE [55]. In order to assess the repeatability of the experimental method as a whole, the process of preparing an agar stabilised water sample and measuring its thermal conductivity was repeated two additional times. For each of these repeat experiments, at least 10 measurements of thermal conductivity were performed at 10 °C intervals between 10 °C and 50 °C. Thermal conductivity measurements were subsequently performed on nanofluids stabilised by agar.

Prior to performing thermal conductivity measurements for the agar stabilised aqueous nanofluids, the measurement system was calibrated against the thermal conductivity reference values reported by ASHRAE for deionised water [55]. The thermal conductivity values measured for deionised water stabilised by agar using HPM of the measurement device were used for the calibration. A polynomial was used as the calibration equation. In order to choose the polynomial degree to use, polynomials of increasing degree were fitted to the data. The fit order at which the variance σ^2, as computed below, showed no further significant decrease, provides the best model [57]:

$$\sigma^2 = \frac{\sum_{i=1}^{N} \varepsilon_i^2}{N - m - 1} \tag{2}$$

where ε_i are the residuals, N is the number of data points, and m is the degree of the polynomial. The coefficients for the polynomials fit to the experimental data, to the reference values, and to the correction equation polynomial, are given in Table 1. Measured arithmetically averaged values of thermal conductivity for the nanofluids were corrected using this calibration equation.

Table 1: Polynomial coefficients. These coefficients are for a 7^{th} degree polynomial of the form: $y(T) = aT^7 + bT^6 + cT^5 + dT^4 + eT^3 + fT^2 + gT + h$, where T is the temperature and has units of °C.

Coefficient	Fit Equation For Measured Data	Fit Equation For Reference Data	Correction Equation
a	$8.337\,403 \times 10^{-14}$	$1.105\,838 \times 10^{-15}$	$-8.226\,819 \times 10^{-14}$
b	$-3.166\,674 \times 10^{-11}$	$-3.613\,341 \times 10^{-13}$	$3.130\,540 \times 10^{-11}$
c	$4.622\,170 \times 10^{-9}$	$3.995\,687 \times 10^{-11}$	$-4.582\,213 \times 10^{-9}$
d	$-3.320\,154 \times 10^{-7}$	$-7.617\,286 \times 10^{-10}$	$3.312\,536 \times 10^{-7}$
e	$1.246\,995 \times 10^{-5}$	$-1.678\,040 \times 10^{-7}$	$-1.263\,776 \times 10^{-5}$
f	$-2.492\,925 \times 10^{-4}$	$2.419\,880 \times 10^{-6}$	$2.517\,124 \times 10^{-4}$
g	$3.725\,686 \times 10^{-3}$	$1.890\,536 \times 10^{-3}$	$-1.835\,149 \times 10^{-3}$
h	$5.628\,157 \times 10^{-1}$	$5.610\,038 \times 10^{-1}$	$-1.811\,897 \times 10^{-3}$

2.5. Statistical Analysis

In order to determine whether measured increases in thermal conductivity for the nanofluids were statistically different relative to the predictions of the Maxwell model, 1-sample 2-sided t-tests were performed for the measured thermal conductivities of each nanofluid at temperatures of 10 °C, 20 °C, 30 °C, 40 °C, and 50 °C, using a significance level of $\alpha = 0.01$. In each instance this analysis tested whether the mean of the measured thermal conductivity values for a given nanofluid at a given temperature (with bias error corrector for using the calibration procedure described in Section 2.4) was statistically different from thermal conductivity predicted by the Maxwell model for the nanofluid at that temperature.

2.6. Preparation of Agar Stabilised Gels

A gel composed of deionised water and 0.5 wt% agar was prepared. This agar concentration was found to be a practical lower limit of agar addition that allowed a gel to be formed. The water was brought to the boil, and while boiling, the agar powder (A1296, Sigma-Aldrich, St. Louis, Missouri, USA) was added and the mixture was thoroughly stirred. When a clear solution was observed, the fluid was allowed to cool slightly, and was then poured into the measurement chamber of the thermal conductivity measurement setup. The solution began to solidify and formed a gel upon cooling below approximately 40 °C. The gel remained stable upon re-heating up to approximately 80 °C. Following testing, the gel was removed from the measurement chamber, and was found to be sufficiently rigid to remain in a cylindrical shape and support its own weight, confirming

that convection currents are unlikely to occur during thermal conductivity measurements. Gels were similarly prepared from the 10 vol% ethylene glycol/water solution, and from the prepared nanofluids using the same procedure.

2.7. Preparation of Nanofluids

Aqueous nanofluids incorporating Al_2O_3 and Cu nanoparticles were prepared. Al_2O_3 nanoparticles were obtained in two different particle sizes to investigate the effect of particle size on nanofluid thermal conductivity. All of the nanoparticles had a purity of 99.9 wt%, and were obtained from SkySpring Nanomaterials, Inc. (Houston, Texas, USA). Details of these particles are given in Table 2.

Table 2: Details of nanoparticles used for preparing nanofluids.

Material	Nominal Mean Particle Size	Product Code
γ-Al_2O_3	20 nm	1330DL
α-Al_2O_3	50 nm	1320DL
Cu	60 nm–80 nm	0821XH

The Al_2O_3 nanofluids were prepared with concentrations of 0.1 vol% and 1.0 vol%, while the Cu nanofluid was prepared with a concentration of 0.1 vol%. The nanofluids were prepared using the two-step method, which is well described in the literature [58, 59]. The two-step method was used because of its low-cost and convenience, and because it is possible to achieve a narrower distribution of particle sizes than with the one-step method. This preparation method involves combining a base fluid (deionised water), nanoparticles, and a surfactant, sonicating the fluid, adjusting the pH, and then re-sonicating the fluid. The nanofluids were prepared in batches of 140 ml volume.

Sodium hexametaphosphate ($(NaPO_3)_6$), which is commonly used as a surfactant in the preparation of nanofluids (e.g. [60, 61]), was added to improve nanofluid stability. Experiments with trial batches of nanofluids prepared with different concentrations of sodium hexametaphosphate revealed that a sodium hexametaphosphate quantity equal to 20 wt% of the nanoparticle mass was optimum for achieving a stable nanofluid (by visual inspection of settling after 2 h). This concentration of sodium hexametaphosphate was therefore used to prepare all nanofluids for thermal

conductivity testing. After adding the surfactant, the nanofluids were sonicated for 30 min using a UP200H probe sonicator (Hielscher Ultrasonics GmbH, Teltow, Germany).

To further stabilise the nanofluids, their pH was adjusted by addition of sodium hydroxide (NaOH) and hydrochloric acid (HCl). In order to achieve optimum dispersion, the pH of the alumina nanofluids was adjusted to 8.0 according to the findings of Zhu et al. [60]. The pH of the copper nanofluid was adjusted to 9.0 according to the findings of Li et al. [52]. After pH adjustment, the nanofluids were again sonicated for a further 30 min. The prepared nanofluids exhibited appreciable stability. Onset of particle settling in prepared test batches was observed with copper nanoparticles after a period of several hours, and was observed with alumina nanoparticles after several weeks. Nanofluid batches prepared for thermal conductivity testing were stabilised by agar directly after the final sonication step.

2.8. Characterisation of Nanoparticles and Nanofluids

A number of characterisation techniques were used to evaluate the physical properties of the nanoparticles and the prepared nanofluids. The size and morphology of the nanoparticles prior to nanofluid synthesis was examined by scanning electron microscopy (SEM). A sample of each nanoparticle type was examined using an FEI Quanta 3D FEG SEM (FEI Ltd., Hillsboro, Oregon, USA). Al_2O_3 nanoparticle samples were sputter coated with a thin layer of gold to prevent electrostatic charging during SEM analysis. The nanoparticle size, morphology, and the agglomeration of nanoparticles in each nanofluid was examined by transmission electron microscopy (TEM). A small liquid sample of each prepared nanofluid was diluted, placed on a Formvar/Carbon TEM grid (200 mesh copper) (AGS162H, Agar Scientific Ltd., Essex, UK), and then dried at room temperature. TEM analysis was performed using an FEI Tecnai™ G2 20 Twin TEM (FEI Ltd., Hillsboro, Oregon, USA). Dynamic light scattering (DLS) was used to characterise the agglomerate size distribution of nanoparticles in the nanofluids. Samples of each nanofluid were diluted in deionised water and analysed using a Zetasizer Nano ZS (Malvern Instruments Ltd., Worcestershire, UK) at 25 °C.

2.9. Thermal Conductivity Predictions of Maxwell's Equation

Thermal conductivity predictions were calculated for each nanofluid using Maxwell's model, given in Eq. (1). Variation in thermal conductivity with temperature for copper was obtained from Moore et al. [62], and variation in thermal conductivity with temperature for alumina was obtained from de Faoite et al. [63, 64].

3. Results

3.1. Nanoparticle and Nanofluid Characteristics

Using SEM and TEM analysis, the nominally 20 nm alumina nanoparticles were found to be approximately spherical in shape and predominantly had diameters of the order of 20 nm. The nominally 50 nm Al_2O_3 particles were found to be spherical with diameters predominantly less than 100 nm. These particles were observed to agglomerate into elongated clusters. The nominally 60 nm–80 nm copper nanoparticles were found to be spherical, with particle diameters predominantly less than 100 nm. However, a few anomalously large particles greater than 1 μm in diameter were also observed. DLS analysis revealed that the nominally 20 nm and 50 nm alumina nanofluids exhibited single peaks in agglomerate size distribution at 252 nm and 410 nm, respectively. The nominally 60 nm–80 nm copper nanofluid exhibited two peaks in agglomerate size distribution at 113 nm and 428 nm.

3.2. Thermal Conductivity Results for Water

The thermal conductivity of deionised water without a stabilising agent was measured at several temperatures between 5 °C and 60 °C using the LPM of the measurement system. The resulting (arithmetically averaged) values for measurements up to 50 °C are plotted in Figure 2. The arithmetic mean values of the measured data at each temperature were within ± 10 % of published reference values for thermal conductivity of deionised water [55], but two of the mean values fell outside ± 5 % of the reference values. The measured values showed significant scatter around the reference values for deionised water. The standard deviations of the measured data at each temperature varied non-monotonically with temperature. These standard deviations varied in magnitude

between $0.0065\,\mathrm{W{\cdot}m^{-1}{\cdot}K^{-1}}$ (at 5 °C) and $0.0795\,\mathrm{W{\cdot}m^{-1}{\cdot}K^{-1}}$ (at 45 °C). This measured dataset is considered indicative only. Repetition of these measurements yielded bias errors and standard deviations of similar magnitude, but the measured bias error and standard deviation at each particular temperature was found to vary between experiments. Above 50 °C the scatter in measured datapoints increased significantly. At 60 °C (off the scale of Figure 2) the bias error between the arithmetic mean of measured values and the reference value was $1.372\,\mathrm{W{\cdot}m^{-1}{\cdot}K^{-1}}$, and the standard deviation of measured values was $0.3101\,\mathrm{W{\cdot}m^{-1}{\cdot}K^{-1}}$. This increase in scatter likely results from a decrease in the viscosity of water with increasing temperature, allowing convection currents to form more readily. When operated in HPM, the measured thermal conductivity values for deionised water showed even more pronounced scatter around the reference values.

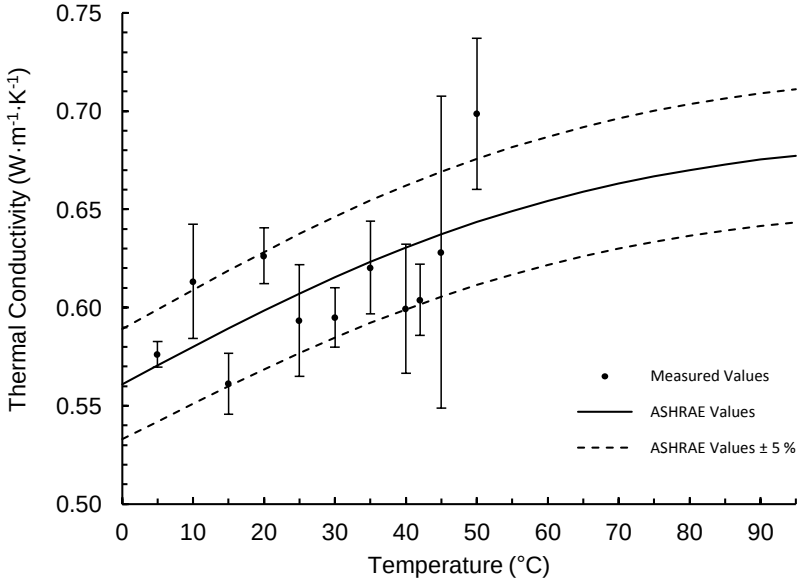

Figure 2: Measured thermal conductivity of deionised water without a stabilising agent at temperatures between 5 °C and 50 °C, measured using low-power mode. Error bars denote one standard deviation above and below the arithmetic mean. Measured values are compared with ASHRAE values, for which ± 5 % bounds are shown [55].

3.3. Thermal Conductivity Results for Water Stabilised by Agar

The thermal conductivity of deionised water stabilised by agar was measured at several temperatures between 5 °C and 70 °C using the LPM of the measurement system. The resulting (arithmetically averaged) values are plotted in Figure 3. The measured data-points were all within ± 5 % of published reference values for thermal conductivity of deionised water [55]. The standard devia-

tions of the measured values at each temperature were found to be between $0.0023\,\mathrm{W{\cdot}m^{-1}{\cdot}K^{-1}}$ and $0.0029\,\mathrm{W{\cdot}m^{-1}{\cdot}K^{-1}}$ up to 50 °C, and increased to $0.0042\,\mathrm{W{\cdot}m^{-1}{\cdot}K^{-1}}$ at 60 °C, and to $0.0075\,\mathrm{W{\cdot}m^{-1}{\cdot}K^{-1}}$ at 70 °C. The higher standard deviation occurring at 70 °C may result from onset of dissolution of the agar gel. Over the studied temperature range the measured thermal conductivity values showed significantly less scatter and lower bias error compared to measurements of water not stabilised by agar.

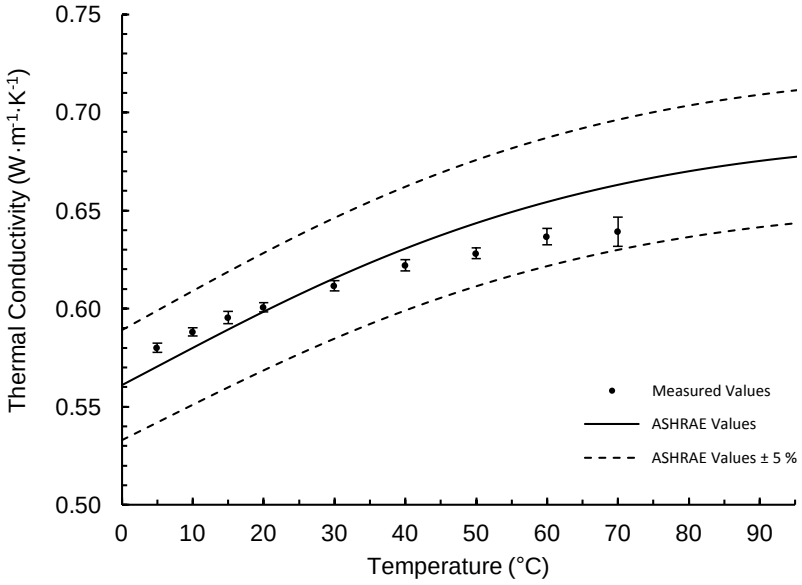

Figure 3: Measured thermal conductivity of deionised water stabilised by agar, at temperatures between 5 °C and 70 °C, measured using low-power mode. Error bars denote one standard deviation above and below the arithmetic mean. Measured values are compared with ASHRAE values, for which ± 5 % bounds are shown [55].

The thermal conductivity of deionised water stabilised by agar was measured at several temperatures between 5 °C and 90 °C using the HPM of the measurement system. The resulting (arithmetically averaged) values are plotted in Figure 4. Up to 80 °C all measured values were all within ± 5 % of published reference values for thermal conductivity of deionised water, with calculated mean values at each temperature within ± 4 % of reference values [55]. The standard deviation of the measurements was found to be between $0.0004\,\mathrm{W{\cdot}m^{-1}{\cdot}K^{-1}}$ and $0.0008\,\mathrm{W{\cdot}m^{-1}{\cdot}K^{-1}}$ up to 80 °C, and increased to $0.0064\,\mathrm{W{\cdot}m^{-1}{\cdot}K^{-1}}$ at 90 °C. The measured values up to 80 °C showed significantly less scatter compared to measurements for water not stabilised by agar, as well as measurements for water stabilised by agar using low-power mode.

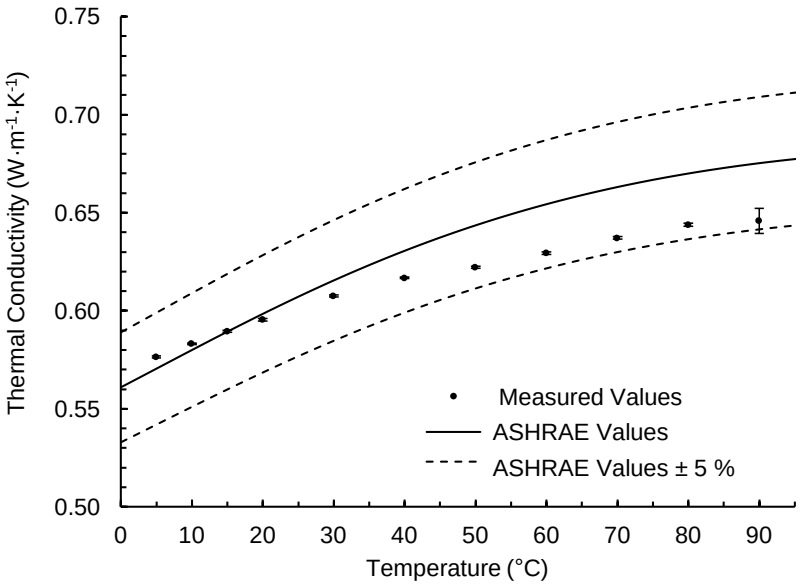

Figure 4: Measured thermal conductivity of deionised water stabilised by agar, at temperatures between 5 °C and 90 °C, measured using high-power mode. Error bars denote one standard deviation above and below the arithmetic mean. Measured values are compared with ASHRAE values, for which ± 5 % bounds are shown [55].

To investigate the repeatability of the experimental method, the process of preparing an agar stabilised water sample and measuring its thermal conductivity was repeated two additional times. For these repeat experiments the HPM of the measurement system was used. 10 measurements at each 10 °C interval between 10 °C and 50 °C were recorded (not shown in Figure 4 for clarity). The three datasets for deionised water stabilised by agar and using HPM were in reasonably good agreement with each other. The bias error between the arithmetic mean of measured values and the reference values over the measured temperature range of 10 °C–50 °C was within ± 3 % for each of the two repeat experiments, similar to the initial measurements performed for agar stabilised water using HPM. The pooled thermal conductivity data for deionised water from these three experiments had standard deviations within $\pm 0.0025\,\mathrm{W{\cdot}m^{-1}{\cdot}K^{-1}}$ between 10 °C and 50 °C. This good agreement indicates that the measurement process as a whole had good repeatability.

3.4. Thermal Conductivity Results for Ethylene Glycol Solution

The thermal conductivity of 10 vol% ethylene glycol/deionised water solution stabilised by agar was measured at several temperatures between 5 °C and 50 °C, using the HPM of the measurement system. The resulting (arithmetically averaged) values are plotted in Figure 5. The measured

data-points were all within ± 2 % of values reported in the literature [55]. The standard deviations of the measurements were found to be between $0.0003\,\mathrm{W{\cdot}m^{-1}{\cdot}K^{-1}}$ and $0.0005\,\mathrm{W{\cdot}m^{-1}{\cdot}K^{-1}}$ over the studied temperature range.

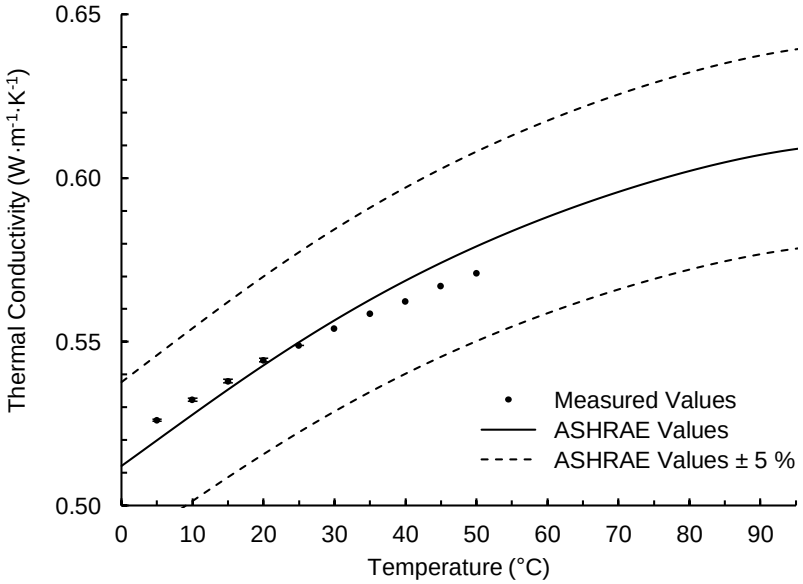

Figure 5: Measured thermal conductivity of 10 vol% EG/deionised water stabilised by agar, at temperatures between 5 °C and 50 °C, measured using high-power mode. Error bars denote one standard deviation above and below the arithmetic mean. Measured values are compared with ASHRAE values, for which ± 5 % bounds are shown [55].

3.5. Measurement System Calibration

Using pooled measured thermal conductivity values from the three datasets for deionised water stabilised by agar and using HPM, the measurement system was calibrated as described in Section 2.4. A 7^{th} degree polynomial was found to be optimal for this dataset, and was fitted to measured data for thermal conductivity of deionised water. The R^2 value for this fit was 0.9934. A 7^{th} degree polynomial was then fitted to the published ASHRAE reference values for thermal conductivity of deionised water, with an R^2 value of 1.0000. The difference between these polynomials was calculated as a function of temperature, and a third polynomial—the correction equation—was fitted to this difference. The coefficients for these three polynomials, are given in the appendix. The correction equation models the bias error in the measurement system, and addition of values from the codomain of this function from measured values at a particular temperature allows this bias error to be corrected for. Measured arithmetically averaged values of thermal conductivity for

the nanofluids were corrected using this correction equation.

3.6. Thermal Conductivity Results for Nanofluids

The thermal conductivities of the prepared nanofluids stabilised by agar were measured as a function of temperature between 10 °C and 50 °C. Due to the lower scatter in measurements obtained when using the HPM of the KD2 Pro device, this power mode was used for measurements of nanofluid thermal conductivity. As with the measurements for deionised water and ethylene glycol/water stabilised by agar and using HPM, the measurements for the nanofluids were found to have very low scatter. Over the studied temperature range measurement standard deviations were between $0.0004\,\mathrm{W{\cdot}m^{-1}{\cdot}K^{-1}}$ and $0.0008\,\mathrm{W{\cdot}m^{-1}{\cdot}K^{-1}}$ for the 0.1 vol% Cu nanofluid, between $0.0009\,\mathrm{W{\cdot}m^{-1}{\cdot}K^{-1}}$ and $0.0031\,\mathrm{W{\cdot}m^{-1}{\cdot}K^{-1}}$ for the 0.1 vol% 20 nm Al_2O_3 nanofluid, between $0.0004\,\mathrm{W{\cdot}m^{-1}{\cdot}K^{-1}}$ and $0.0018\,\mathrm{W{\cdot}m^{-1}{\cdot}K^{-1}}$ for the 0.1 vol% 50 nm Al_2O_3 nanofluid, between $0.0004\,\mathrm{W{\cdot}m^{-1}{\cdot}K^{-1}}$ and $0.0006\,\mathrm{W{\cdot}m^{-1}{\cdot}K^{-1}}$ for the 1.0 vol% 20 nm Al_2O_3 nanofluid, and between $0.0004\,\mathrm{W{\cdot}m^{-1}{\cdot}K^{-1}}$ and $0.0005\,\mathrm{W{\cdot}m^{-1}{\cdot}K^{-1}}$ for the 1.0 vol% 50 nm Al_2O_3 nanofluid. The calibration correction equation was applied to these measured data for nanofluids stabilised by agar as well as to the pooled measured data for deionised water stabilised by agar, to correct for bias error. The resulting data are plotted in Figure 6. Measurement standard deviations are not plotted in Figure 6 for visual clarity.

Table 3 gives the arithmetically averaged mean values of measured thermal conductivity for water and the studied nanofluids as a function of temperature, with the calibration correction equation applied to remove bias error.

Table 4 lists the apparent thermal conductivity increases, calculated as percentages, for the nanofluids relative to the thermal conductivity of the water base fluid:

$$\left(\frac{k_{\mathrm{ex}} - k_{\mathrm{b}}}{k_{\mathrm{b}}}\right) \times 100\,\% \tag{3}$$

where k_{ex} is the mean value of the experimentally measured nanofluid thermal conductivity values at each temperature and k_{b} is the thermal conductivity of the base fluid at that temperature.

The thermal conductivity values for the nanofluids predicted by Maxwell's model are given in

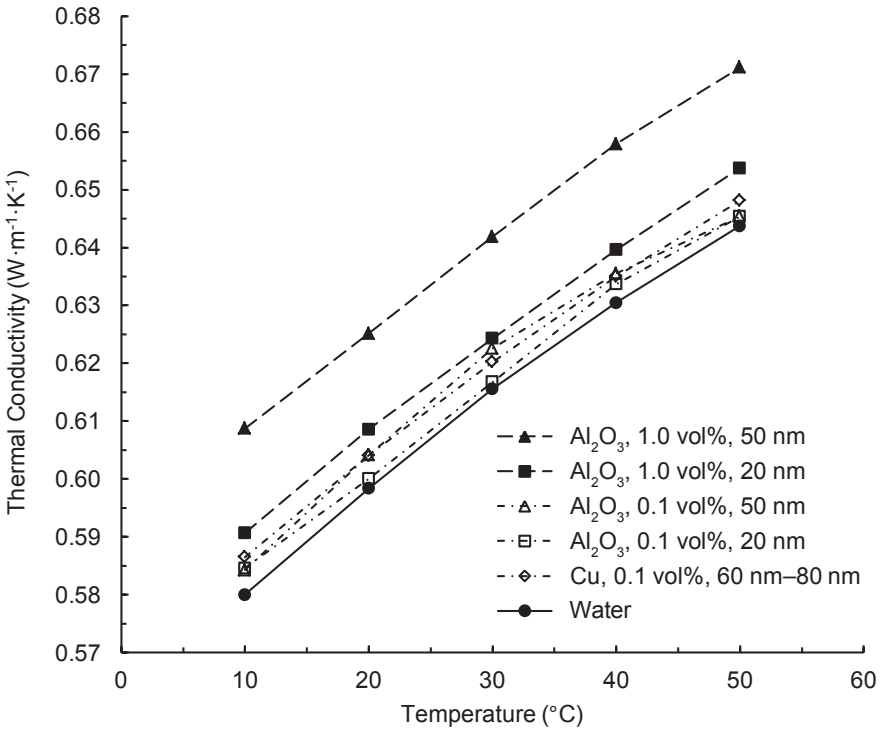

Figure 6: Measured thermal conductivity for deionised water and nanofluids stabilised by agar, at temperatures between 10 °C and 50 °C, measured using high-power mode, and corrected using the calibration equation.

Table 5. Table 6 lists the thermal conductivity increases relative to the water base fluid predicted by Maxwell's model, calculated as percentages:

$$\left(\frac{k_{\mathrm{n}} - k_{\mathrm{b}}}{k_{\mathrm{b}}}\right) \times 100\,\% \tag{4}$$

where k_{n} is the nanofluid thermal conductivity predicted by Maxwell's model at each temperature and k_{b} is the thermal conductivity of the base fluid at that temperature.

Table 7 lists the relative discrepancies between the measured thermal conductivity values for the nanofluids and the thermal conductivities predicted by Maxwell's model, relative to the thermal conductivities predicted by Maxwell's model:

$$\left(\frac{k_{\mathrm{ex}} - k_{\mathrm{n}}}{k_{\mathrm{n}}}\right) \times 100\,\% \tag{5}$$

In this table, values in bold typeface are statistically different ($p < 0.01$) from values predicted by

Table 3: Measured thermal conductivities for the studied nanofluids and deionised water stabilised by agar, with bias error corrector for using the calibration correction equation.

T	Water	Cu 60 nm–80 nm 0.1 vol%	Al_2O_3 20 nm 0.1 vol%	Al_2O_3 50 nm 0.1 vol%	Al_2O_3 20 nm 1.0 vol%	Al_2O_3 50 nm 1.0 vol%
(°C)	($W \cdot m^{-1} \cdot K^{-1}$)					
10	0.5800	0.5865	0.5846	0.5843	0.5907	0.6087
20	0.5984	0.6041	0.6001	0.6041	0.6086	0.6252
30	0.6156	0.6202	0.6168	0.6226	0.6243	0.6419
40	0.6304	0.6350	0.6337	0.6355	0.6396	0.6579
50	0.6438	0.6481	0.6454	0.6454	0.6538	0.6711

Table 4: Measured thermal conductivity increases (in %) for the studied nanofluids.

T	Cu 60 nm–80 nm 0.1 vol%	Al_2O_3 20 nm 0.1 vol%	Al_2O_3 50 nm 0.1 vol%	Al_2O_3 20 nm 1.0 vol%	Al_2O_3 50 nm 1.0 vol%
(°C)	(%)				
10	1.12	0.79	0.73	1.84	4.95
20	0.95	0.28	0.96	1.71	4.48
30	0.75	0.19	1.14	1.42	4.27
40	0.73	0.51	0.80	1.46	4.36
50	0.68	0.25	0.25	1.55	4.25

Maxwell's model.

The measured thermal conductivities for the nanofluids at 20 °C (with bias error corrected for using the calibration correction equation) are plotted in Figure 7 along with the thermal conductivity values predicted by the Maxwell model at 20 °C.

Table 5: Thermal conductivity values predicted by Maxwell's model for the studied nanofluids.

T	Cu 60 nm–80 nm 0.1 vol%	Al_2O_3 20 nm 0.1 vol%	Al_2O_3 50 nm 0.1 vol%	Al_2O_3 20 nm 1.0 vol%	Al_2O_3 50 nm 1.0 vol%
(°C)			($W \cdot m^{-1} \cdot K^{-1}$)		
10	0.5817	0.5817	0.5817	0.5967	0.5967
20	0.6002	0.6001	0.6001	0.6155	0.6155
30	0.6174	0.6173	0.6173	0.6332	0.6332
40	0.6323	0.6322	0.6322	0.6484	0.6484
50	0.6457	0.6456	0.6456	0.6620	0.6620

Table 6: Thermal conductivity increases predicted by Maxwell's model for the studied nanofluids relative to the water base fluid.

T	Cu 60 nm–80 nm 0.1 vol%	Al_2O_3 20 nm 0.1 vol%	Al_2O_3 50 nm 0.1 vol%	Al_2O_3 20 nm 1.0 vol%	Al_2O_3 50 nm 1.0 vol%
(°C)			(%)		
10	0.299	0.285	0.285	2.876	2.876
20	0.299	0.284	0.284	2.865	2.865
30	0.299	0.283	0.283	2.855	2.855
40	0.299	0.282	0.282	2.845	2.845
50	0.299	0.281	0.281	2.835	2.835

Table 7: Relative discrepancies between measured thermal conductivity values and thermal conductivity values predicted by Maxwell's model for the studied nanofluids. Values in bold typeface are statistically different ($p < 0.01$) from values predicted by the Maxwell model.

T	Cu 60 nm–80 nm 0.1 vol%	Al_2O_3 20 nm 0.1 vol%	Al_2O_3 50 nm 0.1 vol%	Al_2O_3 20 nm 1.0 vol%	Al_2O_3 50 nm 1.0 vol%
(°C)			(%)		
10	0.82	0.51	0.45	-1.01	2.01
20	0.65	0.00	0.68	-1.13	1.57
30	0.45	-0.09	0.85	-1.40	1.38
40	0.43	0.23	0.52	-1.35	1.47
50	0.38	-0.03	-0.03	-1.25	1.38

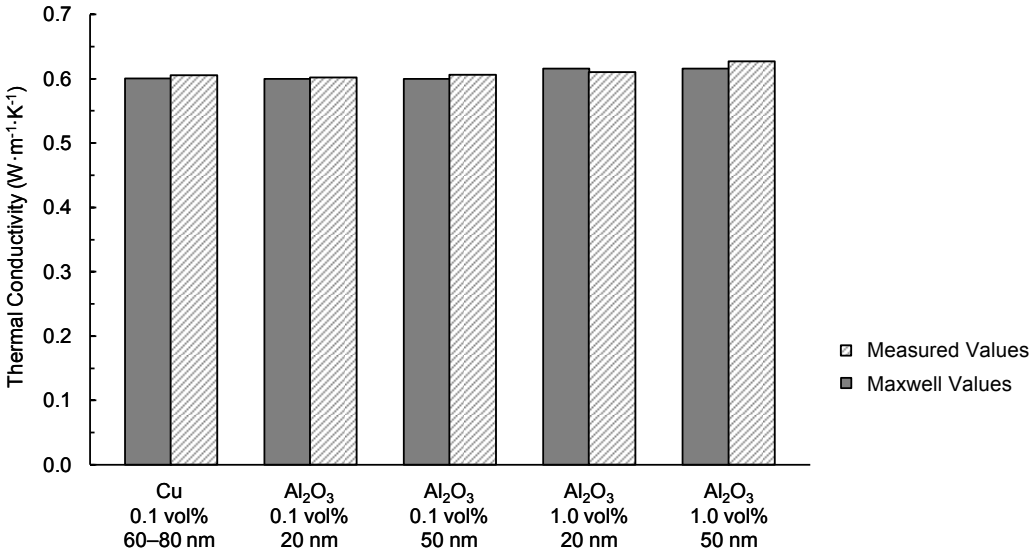

Figure 7: Measured thermal conductivities for nanofluids at 20 °C (hatched columns) compared to thermal conductivity values predicted by the Maxwell model (filled columns) at 20 °C.

4. Discussion

4.1. Thermal Conductivity Measurement Method

For the investigated KD2 Pro/KS-1 measurement system operated in LPM, below 45 °C the arithmetic mean values of thermal conductivity for deionised water not stabilised by agar were within ± 5 % of reference values at all but one temperature (10 °C). This is in broad agreement with the design uncertainty of the KD2 Pro device of ± 5 % as evaluated by the instrument manufacturer. However, individual measured values of thermal conductivity deviated significantly from the published reference values, at some temperatures by more than ± 10 %. The large scatter in measurements is attributable to formation of convection currents in the fluid in an uncontrolled and unpredictable manner. The most repeatable results were obtained below 45 °C, where the fluid viscosity is higher. Above 45 °C, the scatter and bias error became very large, resulting from a decrease in the viscosity of water with increasing temperature, allowing convection currents to form more readily. This finding is in reasonable agreement with the guidelines of the KD2 Pro manufacturer, who state that the practical upper limit for accurate measurement of thermal conductivity of aqueous solutions is ≈ 50 °C [29]. When operated in HPM, the measured thermal conductivity values for water not stabilised by agar showed even more pronounced scatter around the reference values, likely caused by increased convection current formation. It should be noted that the use of HPM with the KD2 Pro/KS-1 system is not recommended by the manufacturer for this reason [54]. Since the measured thermal conductivity values for deionised water would be used as reference values for determining the conductivity enhancements of the nanofluids, inaccuracy in these measurements would cause difficulties in quantifying the thermal conductivity enhancements, especially if the enhancements were below 10 %.

The experimental measurement setup, as described in Section 2.2, was carefully designed to hold the measurement probe securely in place in a test fluid sample free from vibrations, and was designed according to recommendations of the KD2 Pro manufacturer. Similarly, the experimental measurement procedure, as described in Section 2.3, was selected according to recommendations of the KD2 Pro manufacturer, and was intended to ensure that the test fluid was at a uniform steady temperature prior to each test. The large scatter in measured thermal conductivities most likely

results from the intrinsic design of the KD2 Pro, rather than details of rest of the measurement apparatus or measurement procedure.

For measurement of the thermal conductivity of low viscosity fluids using the transient hot-wire method, it is advisable to use a short heating period in order to minimise convection current formation. The thermal conductivity of liquids can be accurately measured if the time over which the conductivity is measured is sufficiently small that convection currents do not form [4]. In the current work, the heating period used was 30 s, which is the minimum heating period for which the KD2 Pro device can be configured. The primary source of measurement uncertainty of the current measurements for water not stabilised by agar is expected to originate from induced fluid motion due to the relatively long heating period intrinsic to the KD2 Pro/KS-1 design.

A measurement system based on the transient hot-wire method composed of the KD2 Pro unit and KS-1 probe has previously been used in numerous studies for the measurement of thermal conductivity of nanofluids [5, 16–25]. However, despite the propensity for convection current formation with the KD2 Pro/KS-1 measurement system, in most published studies the potential deficiencies of this device are not raised as an issue. Only a few studies could be identified that noted the potential for convection current formation with this measurement system due to the long heating period; e.g., Buongiorno et al. [3].

In addition to increasing measurement scatter, formation of convection currents can lead to an upward bias in measured thermal conductivity if the measurement system is not calibrated. Induced bias error can be a non-linear function of temperature. However, the KD2 Pro/KS-1 is factory calibrated at only a single temperature ($\approx 23\,^{\circ}\mathrm{C}$) against glycerol. Many studies of nanofluid thermal conductivity using this measurement system do not mention whether the accuracy of the device was verified or calibrated against a reference fluid. Of particular note, many studies that state the design uncertainty of the device as being $\pm 5\,\%$ report increases in thermal conductivity for nanofluids that are less than this uncertainty level, without performing statistical analysis to determine whether such increases are statistically significant or not.

4.2. Thermal Conductivity Measurement Using Agar as a Stabilising Agent

As a result of the large scatter in measured thermal conductivity values for deionised water, the use of agar as a stabilising agent—as suggested by the manufacturer of the KD2 Pro device [29]—was investigated in the current work as a potential solution.

Measurements of the thermal conductivity of deionised water using agar as a stabilising agent, and using LPM of the KD2 Pro device resulted in significantly reduced scatter in thermal conductivity measurements. The reduction in scatter is attributable to the gelling action of agar, eliminating convection currents.

With LPM of the KD2 Pro device the heat input to the probe is small in order to limit convection current formation. As noted in Section 2.3, for deionised water, LPM results in a temperature rise in the probe of circa 0.3 °C. With the KD2 Pro device operated in HPM, the heat input to the probe is increased, resulting in a higher temperature rise in the probe—circa 3.0 °C for deionised water. With a higher temperature rise in the fluid the relative uncertainty of measurement of this temperature change decreases, leading to increased precision in measurement of the thermal conductivity. HPM cannot be used for low viscosity fluids since it would induce significant convection currents. However, HPM can be used with fluids stabilised by the addition of agar, as convection currents are prevented. Such an increase in thermal conductivity measurement precision would be advantageous for measuring very small thermal conductivity enhancements as may occur with low concentration nanofluids (expected to be less than 1 % for very low concentrations of nanofluids).

Measurements of the thermal conductivity of deionised water stabilised by agar, and using HPM of the KD2 Pro device resulted in reduced measurement scatter up to 80 °C compared to measurements performed without a stabilising agent, or with the use of a stabilising agent using LPM. Measurement standard deviations over the studied temperature range were of the same order of magnitude as the KD2 Pro device resolution of $0.001\,\mathrm{W{\cdot}m^{-1}{\cdot}K^{-1}}$. It should also be noted that stabilisation of the fluid by agar also extends the temperature range over which precise thermal conductivity measurements can be performed. Above 80 °C the scatter in measured thermal conductivity values increased, likely caused by re-dissolution of the agar/water gel.

The two repeat experiments, consisting of preparing agar stabilised water samples and mea-

suring their thermal conductivity, indicated that the experimental method as a whole has good repeatability. The good precision and repeatability achieved using HPM enables the comparison between different nanofluids with thermal conductivities close to that of water.

As a result of the repeatability of measurements obtained for agar stabilised water using HPM, HPM was used for thermal conductivity measurements of the other agar stabilised reference fluid and agar stabilised nanofluids.

To verify the accuracy and repeatability of this measurement method, the thermal conductivity of a 10 vol% ethylene glycol/water solution, stabilised by agar, was also measured and compared to published reference values. Measured thermal conductivity values had standard deviations not exceeding $0.0005\,\mathrm{W{\cdot}m^{-1}{\cdot}K^{-1}}$ over the studied temperature range of 10 °C–50 °C. The (un-calibrated) discrepancy between measured and reference values over this temperature range was within ± 2 %.

The low scatter and moderate bias error of thermal conductivity measurements for agar stabilised water and ethylene glycol/water solution verified the efficacy of using agar as a stabilising agent for thermal conductivity measurement with the transient hot-wire technique.

The bias error present in the measurements is not unexpected as the measurement system was factory-calibrated at a single temperature (≈ 23 °C) in glycerol. Indeed, the bias errors for the measurements of water and 10 vol% EG/water stabilised by agar are small near 23 °C. The bias error of the measurement system was corrected for by calibrating against published reference values reported for the thermal conductivity of water. The un-weighted measurements from each of the 3 experiments for water stabilised by agar using HPM were pooled and used for calculation of the calibration equation. The introduction of 0.5 wt% agar to water to form a gel may slightly alter its thermal conductivity. However, the un-calibrated measurements of thermal conductivity for deionised water stabilised by agar, both using LPM and HPM, were in good agreement with published reference values, indicating that any such change is small. Any perturbation of the thermal conductivity of water caused by addition of agar would in any case be corrected for by calibrating against published reference values for thermal conductivity of water.

The use of a stabilising agent for nanofluid thermal conductivity measurement may also be useful with other thermal conductivity measurement techniques such as the transient plane source or 3ω

method [65], as well as steady state techniques such as the steady state parallel plate method [66].

4.3. Measurement System Uncertainty

The uncertainty of the measurement system must be given some consideration. The uncertainty of a measurement system may be obtained from: (i) a mathematical combination of the uncertainty U_i of each individual component of a measurement system, (ii) obtained from the measurement system manufacturer, or, (iii) calculated from measured data for a reference material (i.e., determined from system calibration).

In the current investigation, a commercially supplied measurement system (the KD2 Pro/KS-1 system) was used, so it was not possible to determine the measurement system uncertainty by combining uncertainties of individual sub-components of this system, as these uncertainties are unknown.

The KD2 Pro/KS-1 manufacturer quotes an uncertainty of $\pm 5\,\%$ for this device (assumed to refer to $\pm 5\,\%$ of the reading value, expressed as a $95\,\%$ confidence interval (CI)). For water at $20\,^{\circ}\mathrm{C}$ ($k \approx 0.598\,\mathrm{W{\cdot}m^{-1}{\cdot}K^{-1}}$) this is equivalent to an uncertainty of $\pm 0.03\,\mathrm{W{\cdot}m^{-1}{\cdot}K^{-1}}$. As noted above, for measurements of the thermal conductivity of water not stabilised by agar using LPM, the measurement standard deviation was of the order of $0.01\,\mathrm{W{\cdot}m^{-1}{\cdot}K^{-1}}$ to $0.03\,\mathrm{W{\cdot}m^{-1}{\cdot}K^{-1}}$ up to $40\,^{\circ}\mathrm{C}$, and increased rapidly above this temperature. The measurements at $40\,^{\circ}\mathrm{C}$, for example, have a $95\,\%$ confidence interval of $0.5994 \pm 0.0176\,\mathrm{W{\cdot}m^{-1}{\cdot}K^{-1}}$. The width of this confidence interval is of the same order of magnitude as the uncertainty quoted by the manufacturer. However, the measurements at $60\,^{\circ}\mathrm{C}$ have a $95\,\%$ CI of $0.8710 \pm 0.1451\,\mathrm{W{\cdot}m^{-1}{\cdot}K^{-1}}$, the width of which exceeds the quoted uncertainty of $\pm 5\,\%$.

For alumina nanofluid with concentrations of 0.1 vol% and 1.0 vol%, the Maxwell model predicts thermal conductivity enhancements of $0.0017\,\mathrm{W{\cdot}m^{-1}{\cdot}K^{-1}}$ and $0.0171\,\mathrm{W{\cdot}m^{-1}{\cdot}K^{-1}}$, respectively, at $20\,^{\circ}\mathrm{C}$. With a measurement instrument with uncertainty of $\pm 0.03\,\mathrm{W{\cdot}m^{-1}{\cdot}K^{-1}}$ ($95\,\%$ CI), it would not be possible to detect such small increases in thermal conductivity, or to determine whether the mean value of a series of measurements for such a nanofluid was significantly higher than the conductivity predicted by the Maxwell model, thereby representing an anomalous increase.

As a result of the modifications of the measurement system—the use of the stabilising

agent agar, and the calibration of the measurement system against reference values for water—determination of the measurement system uncertainty from measured experimental values is more appropriate than using the uncertainty reported by the KD2 Pro/KS-1 manufacturer. Indeed, these modifications were made specifically to reduce the uncertainty of measured values.

As noted in Section 2.5, in order to determine whether measured increases in thermal conductivity for the nanofluids were statistically significant different relative to the predictions of the Maxwell model, 1-sample 2-sided t-tests were performed, using a significance level of $\alpha = 0.01$.

It should be noted that very few studies of nanofluid thermal conductivity report how their measurement system was calibrated against reference fluids. It is also of note that some studies utilising the KD2 Pro/KS-1 system report thermal conductivity enhancements that are within the error bounds quoted for the KD2 Pro/KS-1 system (± 5 %).

4.4. Thermal Conductivity Results for Nanofluids

Thermal conductivity was experimentally measured for the prepared nanofluids with the same procedure used for the reference fluids, using agar as a stabilising agent and using high power mode of the measurement device. The measured values were compared with the predicted thermal conductivity values from Maxwell's model.

All three of the 0.1 vol% nanofluids had measured thermal conductivities higher than that for water. Of these 0.1 vol% nanofluids, the 50 nm alumina and 60 nm–80 nm copper nanofluids had higher measured thermal conductivities than the 20 nm nanofluid. The 50 nm alumina nanofluids had higher thermal conductivity enhancements compared to 20 nm alumina nanofluids for both 0.1 vol% and 1 vol% concentrations. As expected from Maxwell's model, the 1.0 vol% alumina nanofluids had higher thermal conductivities than the 0.1 vol% alumina nanofluids. The highest measured thermal conductivities are seen in nanofluids with loading of 1.0 vol%.

The relative discrepancies between the observed and predicted conductivity enhancement for each nanofluid as a function of temperature are shown in Table 7. For the 0.1 vol% nanofluids the relative discrepancy is within ± 1.0 %. The highest relative discrepancy occurs for the 1.0 vol% 50 nm alumina nanofluid. Surprisingly, for the 1.0 vol% 20 nm alumina nanofluid the measured thermal conductivity is lower than the predicted value over the studied temperature range. The

reason for this is not known, but may result from non-optimal dispersion of nanoparticles in this nanofluid.

For the 0.1 vol% Cu nanofluid, 0.1 vol% 50 nm Al_2O_3 nanofluid, and 1.0 vol% Al_2O_3 nanofluids, the statistical analysis revealed that the mean value of measured thermal conductivity was statistically higher than the value predicted by Maxwell's model at the 0.01 level of significance ($P < 0.01$), with the exception of the measured value for the 0.1 vol% 50 nm Al_2O_3 nanofluid at 50 °C, for which no significant increase was observed. These statistically significant conductivity enhancements relative to the Maxwell model constitute anomalous thermal conductivity enhancements. For the 0.1 vol% 20 nm Al_2O_3 nanofluid no statistical difference between the mean measured value and Maxwell prediction was observed. Surprisingly, for the 1.0 vol% 20 nm Al_2O_3 nanofluid, the mean measured thermal conductivity was found to be statistically lower than the conductivity predicted by the Maxwell model over the studied range of temperatures. It should be noted that although statistical differences were found between measured values and predictions of the Maxwell model, these differences are small in all cases, as illustrated in Figure 7.

Given the simple nature of the Maxwell model, it is not surprising that there is disagreement with the measured values. The Maxwell model does not take account of interaction among particles, or particle shape or aspect ratio [67]. Although the Maxwell model works satisfactorily at low volume concentrations, its predictions do not agree well with most measurements of thermal conductivity for nanofluids reported in the literature. Thermal conductivity enhancement is influenced by numerous factors, including particle shape, size, material, concentration, base fluid, type and concentration of surfactant, pH of the fluid, dispersing method, and Zeta potential [68–70]. As a result of this complexity, significant disagreement exists in the literature about the thermal conductivity enhancement provided by nanofluids.

Ghozatloo et al., for example, studied aqueous nanofluids containing carbon nanotubes and reported thermal conductivity enhancements of 24.9 % and 8.0 % for a single CNT concentration of 0.1 wt% using two different dispersing methods [39]. Numerous studies have reported very large increases in thermal conductivity with the addition of nanoparticles to a base fluid. For instance, a 160 % increase in thermal conductivity was reported by Choi et al. for a nanofluid containing

1 vol% carbon nanotubes [46]. As a result of some of these very high and, according to classical theory, anomalous enhancements, heat transfer nanofluids became the subject of intense research and some controversy emerged as to the real enhancement values and possible underlying heat transfer mechanisms at the nanoscale.

A number of possible mechanisms have been proposed to explain the anomalous thermal conductivity enhancement of nanofluids. These mechanisms include Brownian motion of nanoparticles [71, 72], nanoparticle aggregation [71, 73, 74], liquid layering [71, 75–77], and thermophoresis [71, 72, 75]. It should be noted that the existence and the significance of these proposed mechanisms have been questioned in some studies [47, 48, 75]. Currently, none of the proposed mechanisms adequately predict the thermal conductivity of nanofluids, since the thermal conductivity enhancement depends on many factors, including the particle material, size and shape of the particle, volume concentration, operating temperature, and particle dispersion [78].

There is significant disagreement in the literature regarding the thermal conductivity enhancement of copper and alumina nanofluids. For example, Masuda et al. investigated the thermal conductivity enhancement of alumina nanofluids [53]. They dispersed γ-Al_2O_3 nanoparticles of mean diameter 13 nm in water with volume fractions of 1.3 vol%, 2.8 vol%, and 4.3 vol% (mass fractions of 5 wt%, 10 wt%, and 15 wt%, respectively), and measured thermal conductivity increases of approximately 10 %, 20 % and 30 % for these nanofluids, respectively, over that of the base fluid (water). Lee et al. studied the thermal conductivity of nanofluids of alumina particles in water and ethylene glycol base fluids [10]. Their measured thermal conductivities for alumina nanofluids containing large agglomerated Al_2O_3 particles coincided with the predictions of the Hamilton-Crosser model. Timofeeva et al. studied alumina nanofluids in water and ethylene glycol base fluids and reported thermal conductivity enhancements that were lower than predicted by the Maxwell model, which was ascribed to agglomeration of nanoparticles [15]. Li et al. studied the thermal conductivity enhancement of Cu-water nanofluids as a function of nanofluid pH and SDBS (sodium dodecylbenzenesulfonate) surfactant concentration [52]. With 0.1 wt% and 0.8 % Cu nanoparticle concentration Li et al. reported thermal conductivity enhancement of up to 10.7 % and 18 %, respectively, with optimal pH and SDBS concentration. Eastman et al. reported a 40 %

increase in thermal conductivity for a Cu-ethylene glycol nanofluid, with the Cu nanoparticles coated with thioglycolic acid, with a nanoparticle concentration of only 0.3 wt% (with size less than 10 nm) [45].

Unlike the majority of studies, a number of more recent publications have reported no significant increase in the thermal conductivity. For instance, Putnam, et al. investigated ethanol-based Au nanofluids and reported no anomalous enhancement in nanofluid thermal conductivity [79]. Similarly, the comprehensive International Nanofluid Property Benchmark Exercise (INPBE) study of nanofluid thermal conductivity found that the thermal conductivity enhancement of most nanofluids could be predicted using the effective medium theory [3].

The nanofluid thermal conductivity enhancements measured in the current study are lower than reported in the majority of studies of aqueous copper and alumina nanofluids. Although these enhancements were found to be statistically higher than the values predicted by the Maxwell model for three of these nanofluids, the enhancements in thermal conductivity are small in absolute terms for all of the investigated nanofluids.

Pumped convection cooling loops are one of the most prominent application areas for nanofluids. Theoretically, an increase in fluid thermal conductivity should increase the heat transfer coefficient in the developing flow region. Similar to reports of anomalous increases in thermal conductivity, numerous studies have reported anomalously large increases in convection heat transfer coefficient [38, 80–93]. Li & Xuan, for example, reported a 60 % increase in heat transfer coefficient in the laminar flow regime with the addition of 2 vol% of copper nanoparticles [80], while Wen & Ding reported a 47 % increase in convection coefficient in the laminar flow regime for alumina nanofluid with a nanoparticle concentration of 1.6 vol% [82]. However, a number of recent studies observed no anomalous increase in heat transfer coefficient for nanofluids [20, 94–97]. As is the case with thermal conductivity, this variation in measured heat transfer coefficient for nanofluids likely results from the dependence of nanofluid thermal transport properties on a larger number of interacting factors, such as particle size, aspect ratio, concentration, and dispersion.

Having a well dispersed and stable nanofluid is of significant importance. An unstable nanofluid will form clusters of agglomerated particles leading to particle settling and a decrease in nanofluid

thermal conductivity [98]. Uniform dispersion of nanoparticles has been highlighted by several studies as being of key importance to the attainment of high thermal conductivity enhancement in nanofluids [98–100]. As noted in Section 2.7, the prepared nanofluids exhibited appreciable stability. Onset of particle settling in prepared test batches was observed with copper nanoparticles after a period of several hours, and with alumina nanoparticles after several weeks. Nanofluid batches prepared for thermal conductivity testing were stabilised by agar directly after the final sonication step. Particle settling is therefore unlikely to have occurred before stabilisation by agar.

Some metallic nanoparticles such as copper have higher thermal conductivities than alumina nanoparticles, but are potentially susceptible to oxidation. In the current study, the thermal conductivity of the copper nanofluid was tested shortly after preparation, minimising the potential for oxidation of the Cu particles.

5. Conclusions

For thermal conductivity measurement of low viscosity fluids using apparatus based on the transient hot-wire method, use of long heating periods can result in formation of convection currents, leading to large scatter in measured conductivity values. Convection current formation becomes more significant with high heat inputs. Addition of agar in a concentration as low as 0.5 wt% to water or an aqueous solution can result in the formation of a gel, preventing the formation of convection currents. The addition of this small mass fraction of agar to water does not significantly change the thermal conductivity. Any small perturbation of the thermal conductivity caused by this addition of agar can be corrected for by calibration of the measurement system against published reference values for thermal conductivity of water. Stabilisation of aqueous solutions and aqueous nanofluids using agar is an effective method to enable the thermal conductivity of these fluids to be accurately and repeatably measured using the transient hot-wire technique. Stabilisation of the fluid in this manner allows a larger heat input to be applied to a hot-wire probe, thereby improving the precision of the thermal conductivity measurements. Furthermore, stabilisation of the fluid allows precise measurements of thermal conductivity to be made up to approximately 80 °C. The use of agar as a stabilising agent, with a moderately high power input to the probe, allows

the thermal conductivity of water to be measured with an uncertainty within $\pm 0.0025\,\mathrm{W{\cdot}m^{-1}{\cdot}K^{-1}}$ ($\pm 1\sigma$) up to 50 °C. The good repeatability obtained with this measurement method allows it to be used to reliably investigate the thermal conductivity enhancement of aqueous nanofluids, including nanofluids containing low concentrations of nanoparticles.

The thermal conductivity enhancements of 0.1 vol% Cu and Al_2O_3, and 1.0 vol% Al_2O_3 nanofluids fall within $\approx \pm 2$ % of values predicted by Maxwell's model. Although statistically significant enhancements in thermal conductivity relative to the predictions of the Maxwell model were observed for 0.1 vol% Cu nanofluid, 0.1 vol% 50 nm Al_2O_3 nanofluid, and 1.0 vol% 50 nm Al_2O_3 nanofluids, in absolute terms the observed thermal conductivity enhancements were low.

References

[1] H. M. Roder, A transient hot-wire thermal-conductivity apparatus for fluids, Journal of Research of the National Bureau of Standards 86 (5) (1981) 457–493. doi:10.6028/jres.086.020.

[2] R. S. Brodkey, H. C. Hershey, Transport Phenomena: A Unified Approach, Brodkey Publishing, 1988.

[3] J. Buongiorno, D. C. Venerus, N. Prabhat, T. McKrell, J. Townsend, R. Christianson, Y. V. Tolmachev, P. Keblinski, L. W. Hu, J. L. Alvarado, I. C. Bang, S. W. Bishnoi, M. Bonetti, F. Botz, A. Cecere, Y. Chang, G. Chen, H. Chen, S. J. Chung, M. K. Chyu, S. K. Das, R. Di Paola, Y. Ding, F. Dubois, G. Dzido, J. Eapen, W. Escher, D. Funfschilling, Q. Galand, J. Gao, P. E. Gharagozloo, K. E. Goodson, J. Gustavo Gutierrez, H. Hong, M. Horton, K. S. Hwang, C. S. Iorio, S. P. Jang, A. B. Jarzebski, Y. Jiang, L. Jin, S. Kabelac, A. Kamath, M. A. Kedzierski, L. G. Kieng, C. Kim, J. H. Kim, S. Kim, S. H. Lee, K. C. Leong, I. Manna, B. Michel, R. Ni, H. E. Patel, J. Philip, D. Poulikakos, C. Reynaud, R. Savino, P. K. Singh, P. Song, T. Sundararajan, E. Timofeeva, T. Tritcak, A. N. Turanov, S. Van Vaerenbergh, D. Wen, S. Witharana, C. Yang, W. H. Yeh, X. Z. Zhao, S. Q. Zhou, A benchmark study on the thermal conductivity of nanofluids, Journal of Applied Physics 106 (9) (2009) 094312. doi:10.1063/1.3245330.

[4] G. Paul, M. Chopkar, I. Manna, P. K. Das, Techniques for measuring the thermal conductivity of nanofluids: A review, Renewable and Sustainable Energy Reviews 14 (7) (2010) 1913–1924. doi:10.1016/j.rser.2010.03.017.

[5] A. Nasiri, M. Shariaty-Niasar, A. M. Rashidi, R. Khodafarin, Effect of CNT structures on thermal conductivity and stability of nanofluid, International Journal of Heat and Mass Transfer 55 (5-6) (2012) 1529–1535. doi:10.1016/j.ijheatmasstransfer.2011.11.004.

[6] J. J. Healy, J. J. de Groot, J. Kestin, The theory of the transient hot-wire method for measuring thermal conductivity, Physica B+C 82 (2) (1976) 392–408. doi:10.1016/0378-4363(76)90203-5.

[7] J. Kestin, W. A. Wakeham, A contribution to the theory of the transient hot-wire technique for thermal conductivity measurements, Physica A: Statistical Mechanics and its Applications 92 (1-2) (1978) 102–116. doi:10.1016/0378-4371(78)90023-7.

[8] Y. Nagasaka, A. Nagashima, Absolute measurement of the thermal conductivity of electrically conducting liquids by the transient hot-wire method, Journal of Physics E: Scientific Instruments 14 (1981) 1435. doi:10.1088/0022-3735/14/12/020.

[9] Y. Nagasaka, A. Nagashima, Simultaneous measurement of the thermal conductivity and the thermal diffusivity of liquids by the transient hot-wire method, Review of Scientific Instruments 52 (1981) 229. doi:10.1063/1.1136577.

[10] S. Lee, S. U. S. Choi, S. Li, J. A. Eastman, Measuring thermal conductivity of fluids containing oxide nanoparticles, Journal of Heat Transfer 121 (2) (1999) 280–289. doi:10.1115/1.2825978.

[11] H. E. Patel, S. K. Das, T. Sundararajan, Thermal conductivities of naked and monolayer protected metal nanoparticle based nanofluids: Manifestation of anomalous enhancement and chemical effects, Applied Physics

Letters 83 (14) (2003) 2931. doi:10.1063/1.1602578.

[12] S. M. S. Murshed, K. C. Leong, C. Yang, Enhanced thermal conductivity of TiO_2-water based nanofluids, International Journal of Thermal Sciences 44 (4) (2005) 367–373. doi:10.1016/j.ijthermalsci.2004.12.005.

[13] C. A. Nieto De Castro, J. C. G. Calado, W. A. Wakeham, M. Dix, An apparatus to measure the thermal conductivity of liquids, Journal of Physics E: Scientific Instruments 9 (12) (1976) 1073–1080. doi:10.1088/0022-3735/9/12/020.

[14] T. K. Hong, H. S. Yang, C. J. Choi, Study of the enhanced thermal conductivity of Fe nanofluids, Journal of Applied Physics 97 (6) (2005) 064311. doi:10.1063/1.1861145.

[15] E. V. Timofeeva, A. N. Gavrilov, J. M. McCloskey, Y. V. Tolmachev, S. Sprunt, L. M. Lopatina, J. V. Selinger, Thermal conductivity and particle agglomeration in alumina nanofluids: Experiment and theory, Physical Review E 76 (2007) 061203. doi:10.1103/PhysRevE.76.061203.

[16] L. Wang, X. Wei, Nanofluids: Synthesis, heat conduction, and extension, Journal of Heat Transfer 131 (3) (2009) 033102. doi:10.1115/1.3056597.

[17] M. Yeganeh, N. Shahtahmasebi, A. Kompany, E. K. Goharshadi, A. Youssefi, L. Šiller, Volume fraction and temperature variations of the effective thermal conductivity of nanodiamond fluids in deionized water, International Journal of Heat and Mass Transfer 53 (15-16) (2010) 3186–3192. doi:10.1016/j.ijheatmasstransfer.2010.03.008.

[18] D. Han, Z. Meng, D. Wu, C. Zhang, H. Zhu, Thermal properties of carbon black aqueous nanofluids for solar absorption, Nanoscale Research Letters 6 (2011) 457. doi:10.1186/1556-276X-6-457.

[19] O. Manna, S. K. Singh, G. Paul, Enhanced thermal conductivity of nano-SiC dispersed water based nanofluid, Bulletin of Materials Science 35 (5) (2012) 707–712. doi:10.1007/s12034-012-0366-7.

[20] A. T. Utomo, H. Poth, P. T. Robbins, A. W. Pacek, Experimental and theoretical studies of thermal conductivity, viscosity and heat transfer coefficient of titania and alumina nanofluids, International Journal of Heat and Mass Transfer 55 (25-26) (2012) 7772–7781. doi:10.1016/j.ijheatmasstransfer.2012.08.003.

[21] S. M. Abbasi, A. Rashidi, A. Nemati, K. Arzani, The effect of functionalisation method on the stability and the thermal conductivity of nanofluid hybrids of carbon nanotubes/gamma alumina, Ceramics International 39 (4) (2013) 3885–3891. doi:10.1016/j.ceramint.2012.10.232.

[22] B. T. Branson, P. S. Beauchamp, J. C. Beam, C. M. Lukehart, J. L. Davidson, Nanodiamond nanofluids for enhanced thermal conductivity, ACS Nano 7 (4) (2013) 3183–3189. doi:10.1021/nn305664x.

[23] L. S. Sundar, M. K. Singh, E. V. Ramana, B. Singh, J. Grácio, A. C. M. Sousa, Enhanced thermal conductivity and viscosity of nanodiamond-nickel nanocomposite nanofluids, Scientific Reports 4 (2014) 4039. doi:10.1038/srep04039.

[24] A. Karimi, M. A. A. Sadatlu, B. Saberi, H. Shariatmadar, M. Ashjaee, Experimental investigation on thermal conductivity of water based nickel ferrite nanofluids, Advanced Powder Technology 26 (6) (2015) 1529–1536. doi:10.1016/j.apt.2015.08.015.

[25] T. Maré, S. Halelfadl, S. Van Vaerenbergh, P. Estellé, Unexpected sharp peak in thermal conductivity of carbon nanotubes water-based nanofluids, International Communications in Heat and Mass Transfer 66 (2015) 80–83. doi:10.1016/j.icheatmasstransfer.2015.05.013.

[26] M. Tako, S. Nakamura, Gelation mechanism of agarose, Carbohydrate Research 180 (2) (1988) 277–284. doi:10.1016/0008-6215(88)80084-3.

[27] M. Tako, Structural principles of polysaccharide gels, Journal of Applied Glycoscience 47 (1) (2000) 49–53. doi:10.5458/jag.47.49.

[28] M. Tako, The principle of polysaccharide gels, Advances in Bioscience and Biotechnology 6 (2015) 22–36. doi:10.4236/abb.2015.61004.

[29] D. R. Cobos, Using the KD2 Pro to measure thermal properties of fluids.

[30] G. S. Campbell, C. Calissendorff, J. H. Williams, Probe for measuring soil specific heat using a heat-pulse method, Soil Science Society of America Journal 55 (1) 291–293. doi:10.2136/sssaj1991.03615995005500010052x.

[31] E. Ochsner, R. Horton, T. Ren, Use of the dual-probe heat-pulse technique to monitor soil water content in the vadose zone, Vadose Zone Journal 2 (4) (2003) 572–579. doi:10.2113/2.4.572.

[32] X. Liu, Evaluation of the heat-pulse technique for measuring soil water content with thermo-TDR sensor, Procedia Environmental Sciences 11 (2011) 1234–1239. doi:10.1016/j.proenv.2011.12.185.

[33] B. Rajabifar, Enhancement of the performance of a double layered microchannel heatsink using PCM slurry and nanofluid coolants, International Journal of Heat and Mass Transfer 88 (2015) 627–635. doi:10.1016/j.ijheatmasstransfer.2015.05.007.

[34] T. C. Hung, W. M. Yan, X. D. Wang, C. Y. Chang, Heat transfer enhancement in microchannel heat sinks using nanofluids, International Journal of Heat and Mass Transfer 55 (9-10) (2012) 2559–2570. doi:10.1016/j.ijheatmasstransfer.2012.01.004.

[35] R. Saidur, K. Y. Leong, H. A. Mohammad, A review on applications and challenges of nanofluids, Renewable and Sustainable Energy Reviews 15 (3) (2011) 1646–1668. doi:10.1016/j.rser.2010.11.035.

[36] W. Jiang, G. Ding, H. Peng, Measurement and model on thermal conductivities of carbon nanotube nanorefrigerants, International Journal of Thermal Sciences 48 (6) (2009) 1108–1115. doi:10.1016/j.ijthermalsci.2008.11.012.

[37] E. Firouzfar, M. Soltanieh, S. H. Noie, S. H. Saidi, Energy saving in HVAC systems using nanofluid, Applied Thermal Engineering 31 (8-9) (2011) 1543–1545. doi:10.1016/j.applthermaleng.2011.01.029.

[38] Y. Ding, H. Alias, D. Wen, R. A. Williams, Heat transfer of aqueous suspensions of carbon nanotubes (cnt nanofluids), International Journal of Heat and Mass Transfer 49 (1-2) (2006) 240–250. doi:10.1016/j.ijheatmasstransfer.2005.07.009.

[39] A. Ghozatloo, A. M. Rashidi, M. Shariaty-Niasar, Effects of surface modification on the dispersion and thermal conductivity of CNT/water nanofluids, International Communications in Heat and Mass Transfer 54 (2014)

1–7. doi:10.1016/j.icheatmasstransfer.2014.02.013.

[40] D. P. Kulkarni, P. K. Namburu, H. Ed Bargar, D. K. Das, Convective heat transfer and fluid dynamic characteristics of SiO_2 ethylene glycol/water nanofluid, Heat Transfer Engineering 29 (12) (2008) 1027–1035. doi:10.1080/01457630802243055.

[41] M. A. Zennifer, S. Manikandan, K. S. Suganthi, V. L. Vinodhan, K. S. Rajan, Development of CuO-ethylene glycol nanofluids for efficient energy management: Assessment of potential for energy recovery, Energy Conversion and Management 105 (2015) 685–696. doi:10.1016/j.enconman.2015.08.015.

[42] E. Ettefaghi, H. Ahmadi, A. Rashidi, A. Nouralishahi, S. S. Mohtasebi, Preparation and thermal properties of oil-based nanofluid from multi-walled carbon nanotubes and engine oil as nano-lubricant, International Communications in Heat and Mass Transfer 46 (2013) 142–147. doi:10.1016/j.icheatmasstransfer.2013.05.003.

[43] D. K. Agarwal, A. Vaidyanathan, S. S. Kumar, Experimental investigation on thermal performance of kerosene-graphene nanofluid, Experimental Thermal and Fluid Science 71 (2016) 126–137. doi:10.1016/j.expthermflusci.2015.10.028.

[44] J. C. Maxwell, A Treatise on Electricity and Magnetism, Vol. 2, Clarendon Press, 1873.

[45] J. A. Eastman, S. U. S. Choi, S. Li, W. Yu, L. J. Thompson, Anomalously increased effective thermal conductivities of ethylene glycol-based nanofluids containing copper nanoparticles, Applied Physics Letters 78 (6) (2001) 718–720. doi:10.1063/1.1341218.

[46] S. U. S. Choi, Z. G. Zhang, W. Yu, F. E. Lockwood, E. A. Grulke, Anomalous thermal conductivity enhancement in nanotube suspensions, Applied Physics Letters 79 (14) (2001) 2252–2254. doi:10.1063/1.1408272.

[47] P. Keblinski, R. Prasher, J. Eapen, Thermal conductance of nanofluids: is the controversy over?, Journal of Nanoparticle Research 10 (7) (2008) 1089–1097. doi:10.1007/s11051-007-9352-1.

[48] K. S. Hong, Thermal conductivity of Fe nanofluids depending on the cluster size of nanoparticles, Applied Physics Letters 88 (3) (2005) 031901. doi:10.1063/1.2166199.

[49] N. R. Karthikeyan, J. Philip, B. Raj, Effect of clustering on the thermal conductivity of nanofluids, Materials Chemistry and Physics 109 (1) (2008) 50–55. doi:10.1016/j.matchemphys.2007.10.029.

[50] A. Nasiri, M. Shariaty-Niasar, A. Rashidi, A. Amrollahi, R. Khodafarin, Effect of dispersion method on thermal conductivity and stability of nanofluid, Experimental Thermal and Fluid Science 35 (4) (2011) 717–723. doi:10.1016/j.expthermflusci.2011.01.006.

[51] S. M. S. Murshed, C. A. Nieto de Castro, M. J. V. Lourenço, Effect of surfactant and nanoparticle clustering on thermal conductivity of aqueous nanofluids, Journal of Nanofluids 1 (2) (2012) 175–179. doi:10.1166/jon.2012.1020.

[52] X. F. Li, D. S. Zhu, X. J. Wang, N. Wang, J. W. Gao, H. Li, Thermal conductivity enhancement dependent pH and chemical surfactant for Cu-H_2O nanofluids, Thermochimica Acta 469 (1-2) (2008) 98–103. doi:10.1016/j.tca.2008.01.008.

[53] H. Masuda, A. Ebata, K. Teramae, N. Hishinuma, Alteration of thermal conductivity and viscosity of liquid

by dispersing ultra-fine particles (Dispersion of Al_2O_3, SiO_2 and TiO_2 ultra-fine particles), Netsu Bussei 7 (4) (1993) 227–233. doi:10.2963/jjtp.7.227.

[54] KD2 pro thermal properties analyzer—operator's manual (2016).

[55] M. S. Owen (Ed.), 2009 ASHRAE Handbook: Fundamentals, American Society of Heating, Refrigeration and Air-Conditioning Engineers, Inc., 2009.

[56] L. F. Cabeza (Ed.), Advances in Thermal Energy Storage Systems, Woodhead Publishing Series in Energy, Woodhead Publishing, 2015. doi:10.1016/B978-1-78242-088-0.50024-9.

[57] C. F. Gerald, P. O. Wheatley, Applied Numerical Analysis, seventh Edition, Pearson Education Inc., 2007.

[58] Y. Li, J. Zhou, S. Tung, E. Schneider, S. Xi, A review on development of nanofluid preparation and characterization, Powder Technology 196 (2) (2009) 89–101. doi:10.1016/j.powtec.2009.07.025.

[59] W. Yu, H. Xie, A review of nanofluids: Preparation, stability mechanisms, and applications, Journal of Nanomaterials 2012 (2012) 435873. doi:10.1155/2012/435873.

[60] D. Zhu, X. Li, N. Wang, X. Wang, J. Gao, H. Li, Dispersion behavior and thermal conductivity characteristics of Al_2O_3-H_2O nanofluids, Current Applied Physics 9 (1) (2009) 131–139. doi:10.1016/j.cap.2007.12.008.

[61] K. S. Suganthi, K. S. Rajan, Temperature induced changes in ZnO-water nanofluid: Zeta potential, size distribution and viscosity profiles, International Journal of Heat and Mass Transfer 55 (25-26) (2012) 7969–7980. doi:10.1016/j.ijheatmasstransfer.2012.08.032.

[62] J. P. Moore, D. L. McElroy, R. S. Graves, Thermal conductivity and electrical resistivity of high-purity copper from 78 to 400 °k, Canadian Journal of Physics 45 (1967) 3849. doi:10.1139/p67-323.

[63] D. de Faoite, D. J. Browne, F. R. Chang-Díaz, K. T. Stanton, A review of the processing, composition, and temperature-dependent mechanical and thermal properties of dielectric technical ceramics, Journal of Materials Science 47 (10) (2012) 4211–4235. doi:10.1007/s10853-011-6140-1.

[64] D. de Faoite, D. J. Browne, K. T. Stanton, Regression analysis of temperature-dependent mechanical and thermal properties of dielectric technical ceramics, Journal of Materials Science 48 (1) (2013) 451–461. doi:10.1007/s10853-012-6759-6.

[65] S. K. Das, N. Putra, P. Thiesen, W. Roetzel, Temperature dependence of thermal conductivity enhancement for nanofluids, Journal of Heat Transfer 125 (4) (2003) 567–574. doi:10.1115/1.1571080.

[66] X. Wang, X. Xu, S. U. S. Choi, Thermal conductivity of nanoparticle-fluid mixture, Journal of Thermophysics and Heat Transfer 13 (4) (1993) 474–480. doi:10.2514/2.6486.

[67] M. M. MacDevette, H. Ribera, T. G. Myers, A simplet yet effective model for thermal conductivity of nanofluids (2013).

[68] M. Chopkar, S. Sudarshan, P. K. Das, I. Manna, Effect of particle size on thermal conductivity of nanofluid, Metallurgical and Materials Transactions A 39 (7) (2008) 1535–1542. doi:10.1007/s11661-007-9444-7.

[69] A. Ghadimi, R. Saidur, H. S. C. Metselaar, A review of nanofluid stability properties and characterization in stationary conditions, International Journal of Heat and Mass Transfer 54 (17-18) (2011) 4051–4068.

doi:10.1016/j.ijheatmasstransfer.2011.04.014.

[70] J. Jeong, C. Li, Y. Kwon, J. Lee, S. H. Kim, R. Yun, Particle shape effect on the viscosity and thermal conductivity of ZnO nanofluids, International Journal of Refrigeration 36 (8) (2013) 2233–2241. doi:10.1016/j.ijrefrig.2013.07.024.

[71] P. Keblinski, S. R. Phillpot, S. U. S. Choi, J. A. Eastman, Mechanisms of heat flow in suspensions of nano-sized particles (nanofluids), International Journal of Heat and Mass Transfer 45 (4) (2002) 855–863. doi:10.1016/S0017-9310(01)00175-2.

[72] J. Koo, C. Kleinstreuer, Impact analysis of nanoparticle motion mechanisms on the thermal conductivity of nanofluids, International Communications in Heat and Mass Transfer 32 (9) (2005) 1111–1118. doi:10.1016/j.icheatmasstransfer.2005.05.014.

[73] R. Prasher, W. Evans, P. Meakin, J. Fish, P. Phelan, P. Keblinski, Effect of aggregation on thermal conduction in colloidal nanofluids, Applied Physics Letters 89 (14) (2006) 143119. doi:10.1063/1.2360229.

[74] W. Evans, R. Prasher, J. Fish, P. Meakin, P. Phelan, P. Keblinski, Effect of aggregation and interfacial thermal resistance on thermal conductivity of nanocomposites and colloidal nanofluids, International Journal of Heat and Mass Transfer 51 (5-6) (2008) 1431–1438. doi:10.1016/j.ijheatmasstransfer.2007.10.017.

[75] M. Chandrasekar, S. Suresh, A review on the mechanisms of heat transport in nanofluids, Heat Transfer Engineering 30 (14) (2009) 1136–1150. doi:10.1080/01457630902972744.

[76] C. Sitprasert, P. Dechaumphai, V. Juntasaro, A thermal conductivity model for nanofluids including effect of the temperature-dependent interfacial layer, Journal of Nanoparticle Research 11 (6) (2009) 1465–1476. doi:10.1007/s11051-008-9535-4.

[77] L. Li, Y. Zhang, H. Ma, M. Yang, Molecular dynamics simulation of effect of liquid layering around the nanoparticle on the enhanced thermal conductivity of nanofluids, Journal of Nanoparticle Research 12 (3) (2010) 811–821. doi:10.1007/s11051-009-9728-5.

[78] L. Godson, B. Raja, D. M. Lal, S. Wongwises, Enhancement of heat transfer using nanofluids—An overview, Renewable and Sustainable Energy Reviews 14 (2) (2010) 629–641. doi:10.1016/j.rser.2009.10.004.

[79] S. A. Putnam, D. G. Cahill, P. V. Braun, Z. Ge, R. Shirrin, Thermal conductivity of nanoparticle suspensions, Journal of Applied Physics 99 (8) (2006) 084308. doi:10.1063/1.2189933.

[80] Q. Li, Y. Xuan, Convective heat transfer and flow characteristics of Cu-water nanofluid, Science in China Series E: Technological Science 45 (4) (2002) 408–416.

[81] Y. Xuan, Q. Li, Investigation of convective heat transfer and flow features of nanofluids, Journal of Heat Transfer 125 (1) (2003) 151–155. doi:10.1115/1.1532008.

[82] D. Wen, Y. Ding, Experimental investigation into convective heat transfer of nanofluids at the entrance region under laminar flow conditions, International Journal of Heat and Mass Transfer 47 (2004) 5181–5188. doi:10.1016/j.ijheatmasstransfer.2004.07.012.

[83] K. S. Hwang, S. P. Jang, S. U. S. Choi, Flow and convective heat transfer characteristics of water-based Al_2O_3

nanofluids in fully developed laminar flow regime, International Journal of Heat and Mass Transfer 52 (1-2) (2009) 193–199. doi:10.1016/j.ijheatmasstransfer.2008.06.032.

[84] D. Kim, Y. Kwon, Y. Cho, C. Li, S. Cheong, Y. Hwang, J. Lee, D. Hong, S. Moon, Convective heat transfer characteristics of nanofluids under laminar and turbulent flow conditions, Current Applied Physics 9 (2) (2009) e119–e123. doi:10.1016/j.cap.2008.12.047.

[85] S. Torii, W. J. Yang, Heat transfer augmentation of aqueous suspensions of nanodiamonds in turbulent pipe flow, Journal of Heat Transfer 131 (4) (2009) 043203. doi:10.1115/1.3072923.

[86] A. Amrollahi, A. M. Rashidi, R. Lotfi, M. Emami Meibodi, K. Kashefi, Convection heat transfer of functionalized MWNT in aqueous fluids in laminar and turbulent flow at the entrance region, International Communications in Heat Transfer 37 (6) (2010) 717–723.

[87] S. M. Fotukian, M. Nasr Esfahany, Experimental investigation of turbulent convective heat transfer of dilute γ-Al_2O_3/water nanofluid inside a circular tube, International Journal of Heat and Fluid Flow 31 (4) (2010) 606–612. doi:10.1016/j.ijheatfluidflow.2010.02.020.

[88] S. M. Fotukian, M. N. Esfahany, Experimental study of turbulent convective heat transfer and pressure drop of dilute CuO/water nanofluid inside a circular tube, International Communications in Heat and Mass Transfer 37 (2) (2010) 214–219. doi:10.1016/j.icheatmasstransfer.2009.10.003.

[89] H. Xie, Y. Li, W. Yu, Intriguingly high convective heat transfer enhancement of nanofluid coolants in laminar flows, Physics Letters A 374 (25) (2010) 2566–2568. doi:10.1016/j.physleta.2010.04.026.

[90] A. R. Sajadi, M. H. Kazemi, Investigation of turbulent convective heat transfer and pressure drop of TiO_2/water nanofluid in circular tube, International Communications in Heat and Mass Transfer 38 (10) (2011) 1474–1478. doi:10.1016/j.icheatmasstransfer.2011.07.007.

[91] A. Zamzamian, S. N. Oskouie, A. Doosthoseini, A. Joneidi, M. Pazouki, Experimental investigation of forced convective heat transfer coefficient in nanofluids of Al_2O_3/EG and CuO/EG in a double pipe and plate heat exchangers under turbulent flow, Experimental Thermal and Fluid Science 35 (3) (2011) 495–502. doi:10.1016/j.expthermflusci.2010.11.013.

[92] L. Godson, B. Raja, D. M. Lal, S. Wongwises, Convective heat transfer characteristics of silver-water nanofluid under laminar and turbulent flow conditions, Journal of Thermal Science and Engineering Applications 4 (3) (2012) 031001. doi:10.1115/1.4006027.

[93] B. A. Bhanvase, M. R. Sarode, L. A. Putterwar, K. A. Abdullah, M. P. Deosarkar, S. H. Sonawane, Intensification of convective heat transfer in water/ethylene glycol based nanofluids containing TiO_2 nanoparticles, Chemical Engineering and Processing: Process Intensification 82 (2014) 123–131. doi:10.1016/j.cep.2014.06.009.

[94] W. Williams, J. Buongiorno, L. W. Hu, Experimental investigation of turbulent convective heat transfer and pressure loss of alumina/water and zirconia/water nanoparticle colloids (nanofluids) in horizontal tubes, Journal of Heat Transfer 130 (4) (2008) 042412. doi:10.1115/1.2818775.

[95] E. B. Haghighi, M. Saleemi, N. Nikkam, Z. Anwar, I. Lumbreras, M. Behi, S. A. Mirmohammadi, H. Poth,

R. Khodabandeh, M. S. toprak, M. Muhammed, B. Palm, Cooling performance of nanofluids in a small diameter tube, Experimental Thermal and Fluid Science 49 (2013) 114–122. doi:10.1016/j.expthermflusci.2013.04.009.

[96] V. Bianco, O. Manca, S. Nardini, K. Vafai (Eds.), Heat Transfer Enhancement With Nanofluids, CRC Press, 2015.

[97] E. B. Haghighi, Single phase convective heat transfer with nanofluids: An experimental approach, Ph.D. thesis (2015).

[98] X. J. Wang, D. S. Zhu, S. Yang, Investigation of pH and SDBS on enhancement of thermal conductivity in nanofluids, Chemical Physics Letters 470 (1-3) (2009) 107–111. doi:10.1016/j.cplett.2009.01.035.

[99] C. Pak, Y. I. Cho, Hydrodynamic and heat transfer study of dispersed fluids with submicron metallic oxide particles, Experimental Heat Transfer: A Journal of Thermal Energy Generation, Transport, Storage, and Conversion 11 (2) (1998) 151–170. doi:10.1080/08916159808946559.

[100] Y. Xuan, Q. Li, Heat transfer enhancement of nanofluids, International Journal of Heat and Fluid Flow 21 (1) (2000) 58–64. doi:10.1016/S0142-727X(99)00067-3.